H_2 Cracking at SiO_2 Defect Centers†

Mirko Vitiello, Nuria Lopez, and Francesc Illas

Departament de Quimica Fisica, Universitat de Barcelona, Marti i Franques 1, 08028 Barcelona, Spain

Gianfranco Pacchioni*

Dipartimento di Scienza dei Materiali, Università di Milano-Bicocca, and Istituto Nazionale per la Fisica della Materia, via R. Cozzi, 53-20125 Milano, Italy

Received: September 10, 1999; In Final Form: November 17, 1999

The interaction of H_2 with the defect sites of the SiO_2 surface has been studied by means of gradient-corrected density functional theory calculations on cluster models. The mechanism of hydrogen dissociation, the energy of reactants and products, and the corresponding activation energies and transition states have been determined for the following defect sites: Si singly occupied sp^3 dangling bonds (E′ centers), ≡Si$^\bullet$; nonbridging oxygen centers (NBO), ≡Si−O$^\bullet$; divalent Si, =Si:; and neutral oxygen vacancies, ≡Si−Si≡. H_2 cracking on the NBO sites is exothermic by ∼0.4 eV and has an energy barrier of ∼0.1 eV (or less considering nonadiabatic effects) which suggest the occurrence of the process even at low temperature. On Si dangling bonds the formation of ≡Si−H and neutral H atom is endothermic and occurs with an activation energy of less than 0.5 eV; the reaction can occur at room temperature. The interaction of molecular hydrogen with the diamagnetic oxygen deficient centers, =Si: and ≡Si−Si≡, leads to the formation of stable ≡Si−H groups with exothermic processes and relatively high activation energies of about 2 eV. Thus, H_2 cracking is predicted to occur at room temperature on paramagnetic defects and only at high temperatures on the diamagnetic centers.

1. Introduction

The interaction of molecular hydrogen with defect sites (in particular dangling bonds) of SiO_2 is a process which plays a fundamental role in several technological applications. The dielectric reliability of gate silicon dioxide films is a crucial issue in the design of metal oxide semiconductor (MOS) devices.[1−4] Charge traps in the SiO_2 films and at the Si/SiO_2 interface states are known to degrade the dielectric response of the films and the performance of the device. It was recognized a long time ago that the main origins of the charge traps in the material are oxygen deficient centers and other related defects; many of them have been characterized through electron spin resonance[5] (ESR) or UV absorption bands.[6] These defect centers can be stabilized both in the bulk and at the surface of silica glasses.

In the semiconductor industry, annealing of the SiO_2 films in a hydrogen-containing atmosphere is used as a standard technique to reduce the concentration of the defects at the Si/SiO_2 interface. Molecular hydrogen is in fact the only species that can be dissolved in the volume of glass in high concentrations and in relatively "soft" conditions because of its high diffusivity. The role of temperature in the process is essential since it has been observed that there is no change in the concentration of oxygen deficient centers (charge traps) when silica is saturated with H_2 at room temperature. On the other hand, it has also been observed that hydrogen in SiO_2 affects the generation of charge traps, making precursors for electron traps through mechanisms that are not yet completely understood. For instance, it has been suggested that if atomic hydrogen is present in SiO_2 it can depassivate the interface by reaction with the bonded hydrogen (in ≡Si−OH or ≡Si−H groups) to form H_2. Recently, it has been found that the addition of hydrogen into buried oxide layers of $Si/SiO_2/Si$ structures results in the formation of mobile H^+ ions which form the basis for a new class of nonvolatile memory devices.[7] The mechanism of formation of the protons is still unclear. Besides microelectronics, hydrogen has been shown to be useful in fiber optics technology since the refractive index of pure and Ge-doped SiO_2 fibers can be greatly enhanced by loading the fiber with H_2.[8]

Despite the considerable technological interest in the mechanism of interaction of molecular hydrogen with SiO_2, the microscopic aspects of the H_2 breaking remain unclear; the field has been recently reviewed by Edwards.[9] It has been suggested that the two major processes responsible for atomic hydrogen formation are

$$\equiv Si^\bullet + H_2 \rightarrow \equiv Si-H + H^\bullet \quad (1)$$

$$\equiv Si-O^\bullet + H_2 \rightarrow \equiv Si-OH + H^\bullet \quad (2)$$

In these two processes, the centers involved are a Si singly occupied sp^3 dangling bond, the E′ center, and a nonbridging oxygen, NBO. On the basis of semiempirical calculations, Stahlbush et al.[3] estimated an activation barrier for reaction 1 of 1.7 eV, a sufficiently high barrier to exclude the E′ center as a likely candidate for H_2 breaking. This conclusion was contrary to a large set of experimental data which indicate that reaction 1 occurs rapidly at room temperature.[10] The activation energy has also been measured experimentally, although slightly different values have been reported for the same process. Li et al.[11] have found $E_a \approx 0.3$ eV in thermal oxides; in a rather accurate kinetic study, Radzig et al.[12] found a larger barrier, $E_a \approx 0.4-0.5$ eV. On the basis of these results, Edwards

† Part of the special issue "Electronic and Nonlinear Optical Materials: Theory and Modeling".

10.1021/jp993214f CCC: $19.00
Published on Web 01/14/2000

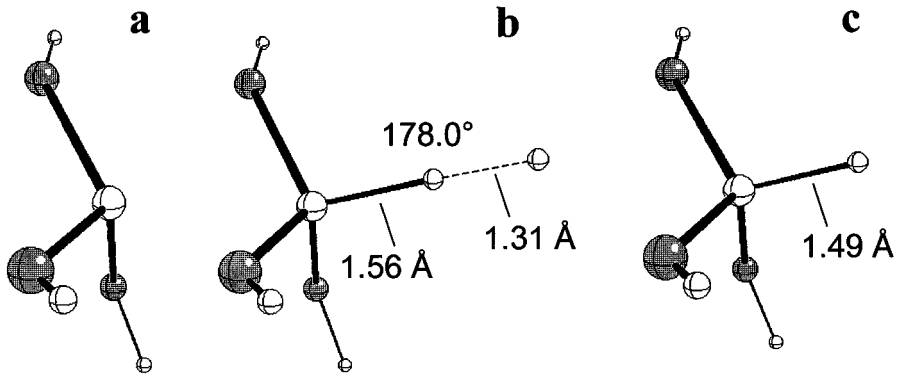

Figure 1. 1-Tetrahedron (1T) cluster model of a Si dangling bond reacting with H_2: (a) $\equiv Si^{\bullet}$ center; (b) transition state $\equiv Si^{\bullet} + H_2$; (c) $\equiv Si-H$ center.

reconsidered the reaction and found $E_a = 0.6-0.7$ eV from ab initio calculations, a value which drops to below 0.2 eV if one includes adiabatic effects.[9] To the best of our knowledge no estimates exist of the activation barrier for reaction 2.

Beside the two paramagnetic centers involved in reactions 1 and 2, other diamagnetic oxygen deficient centers in silica can in principle play a role in the reaction with hydrogen, the dicoordinated Si, $=Si:$, and the neutral oxygen vacancy, $\equiv Si-Si\equiv$ or V_O. In this case, the reactions of interest are

$$=Si: + H_2 \rightarrow =Si(H)_2 \rightarrow \equiv Si-H + H^{\bullet} \quad (3)$$

$$\equiv Si-Si\equiv + H_2 \rightarrow \equiv Si-H + H-Si\equiv \quad (4)$$

Very similar variants of these defects ($\equiv Si^{\bullet}$, $\equiv Si-O^{\bullet}$, $=Si:$, and $\equiv Si-Si\equiv$) are present in bulk amorphous silica and α-quartz,[6] on the surface of mechanically activated silica,[13] in SiO_2 thin films,[14] and in UHV cleaved α-quartz single crystals after Ar^+ bombardment.[15] Fingerprints of the presence of the defect centers on the surface are typical EPR signals and hyperfine coupling constants of the unpaired electron with the ^{29}Si and ^{17}O nuclear spins (E′ and NBO) but also characteristic absorption bands at 5.8 eV (E′), 2 eV (NBO), 5.0 eV (dicoordinated Si), and 7.6 eV (V_O) in the optical spectra of the material.[6] These defect centers are probably the primary cause of the hydrogen dissociation in the oxide or at surfaces.

The object of this paper is to elucidate the role played by the defects described above in the hydrogen breaking in silica. In particular, we have performed high quality quantum mechanical calculations based on cluster models and gradient corrected density functional theory, GC-DFT. The relative stabilities of the reactants and the products and the corresponding energy barriers and transition states have been determined. The results have been checked as a function of the size of the clusters used in the calculations and provide a firm energetic basis for the interpretation of the complex reaction pathways of neutral hydrogen in silica.

2. Computational Approach

To describe point defects in SiO_2, we used cluster models with structures that are derived from that of α-quartz (the Si−O−Si angles in the crystal are 144°, while values in a range of 130−160° are observed in the glassy material).[16] The cluster broken bonds were saturated by H atoms placed at 0.98 Å along the O−Si bond directions of the perfect crystal. The H atoms were kept fixed during the geometrical optimization to provide a simple representation of the mechanical embedding in the solid matrix. In a previous study on the interaction of Cu atoms with similar defect centers at the SiO_2 surface, we used a mixed quantum mechanical molecular mechanics approach.[17] The results have shown that in general even relatively small clusters provide answers similar to those of larger or more complex models where part of the lattice relaxation is treated based on parametrized force fields. Here we have considered the convergence of our results versus cluster size and we have found very similar results with small or large clusters, suggesting that the nature of the interaction is markedly local. As an additional proof of the validity of the cluster model approach for the study of point defects in silica, we mention that very similar structural, electronic, and energetic descriptions of dia- and paramagnetic defects in SiO_2 have been obtained with quantum chemical cluster models using atomic basis functions[18−20] and with ab initio molecular dynamics periodic approaches using plane waves.[21,22] The cluster approach has also been successfully applied to the study of optical transitions in silica.[23−27] Since most of the properties associated with point defects in SiO_2 are local and do not depend markedly on the long range order,[17−27] results obtained from models of α-quartz can be transferred to amorphous silica with some confidence.

The E′ center, $\equiv Si^{\bullet}$, was described by a $(HO)_3Si^{\bullet}$ unit, Figure 1a, including only one Si atom. Since each Si in SiO_2 has a tetrahedral coordination, we denote this cluster as 1T. A larger model, $[(HO)_3SiO]_3Si^{\bullet}$, Figure 2a, contains four Si atoms and is denoted as 4T. In a similar way, we used two cluster models of the $\equiv Si-O^{\bullet}$ groups $(HO)_3Si-O^{\bullet}$, 1T, Figure 3a, and $[(HO)_3SiO]_3Si-O^{\bullet}$, 4T, Figure 4a. Given the similar results obtained with the 1T and 4T models (see below), we used only a small cluster, $(HO)_2Si$, to model the dicoordinated Si, $=Si:$, Figure 5a. The neutral oxygen vacancy, $\equiv Si-Si\equiv$, has been represented by two clusters, a small one, $(HO)_3Si-Si(OH)_3$, Figure 6a, and a larger two-rings cluster, Figure 7a. Full geometry optimizations have been performed by means of analytical gradients of the total energy with the only constraint of keeping the embedding H atoms fixed.

The electronic structure of the cluster has been computed by performing gradient corrected density functional theory (GC-DFT) calculations (spin polarized for open shell cases) using the Becke's three parameters hybrid nonlocal exchange functional[28] combined with the Lee−Yang−Parr gradient-corrected correlation functional[29] (B3LYP). The basis sets used are 6-31G* (a double-ζ plus d polarization function) on Si and on O atoms, 6-31G** (a double-ζ basis with a p polarization function) on the H_2 molecule, and 3-21G on the saturating H atoms of the cluster.[30,31] The use of a hybrid GC-DFT approach guarantees that the energetic is described very accurately. In fact, B3LYP calculations have been shown to reproduce thermodynamic quantities for a large class of molecular systems with great accuracy.[32] However, several uncertainties are

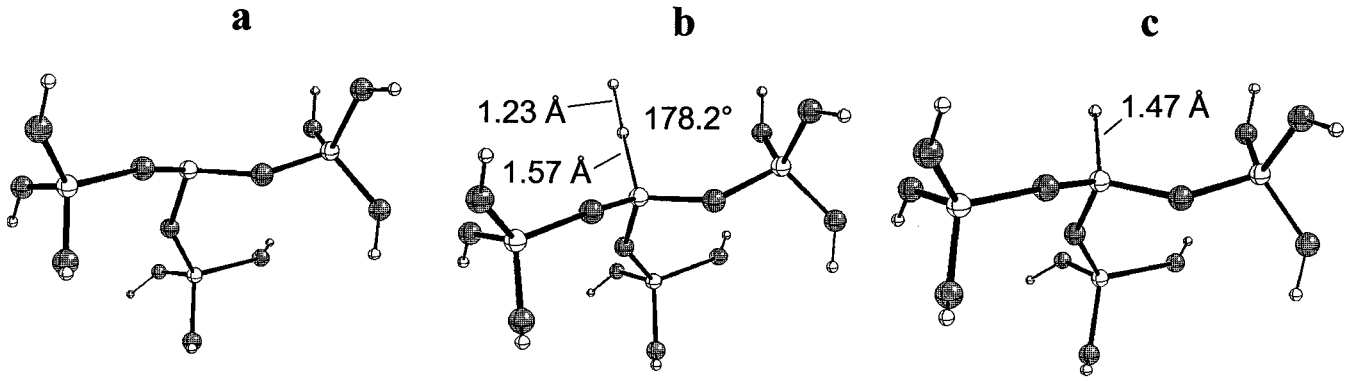

Figure 2. 4-Tetrahedron (4T) cluster model of a Si dangling bond reacting with H_2: (a) ≡Si• center; (b) transition state ≡Si• + H_2; (c) ≡Si−H center.

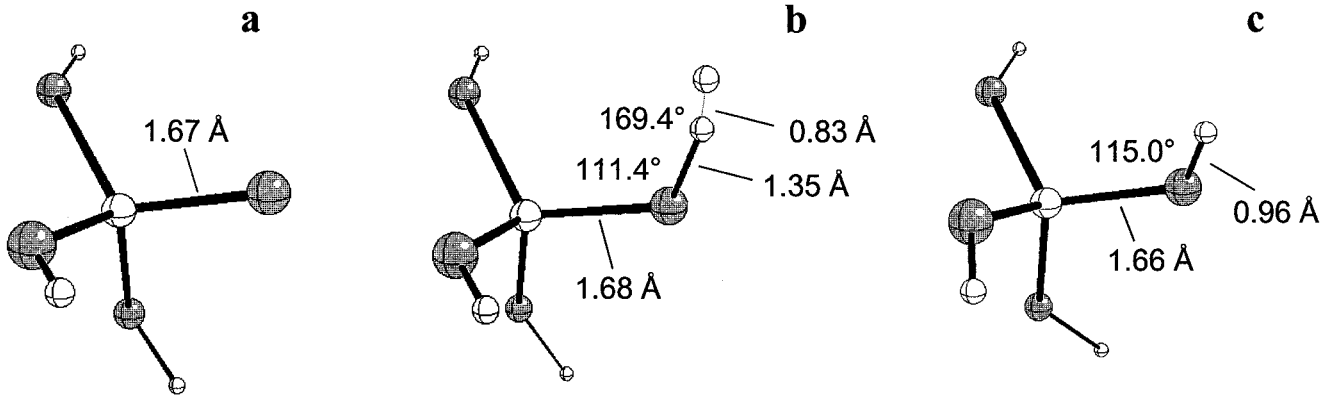

Figure 3. 1-Tetrahedron (1T) cluster model of a nonbridging oxygen (NBO) reacting with H_2: (a) ≡Si−O• center; (b) transition state ≡Si−O• + H_2; (c) ≡Si−OH center.

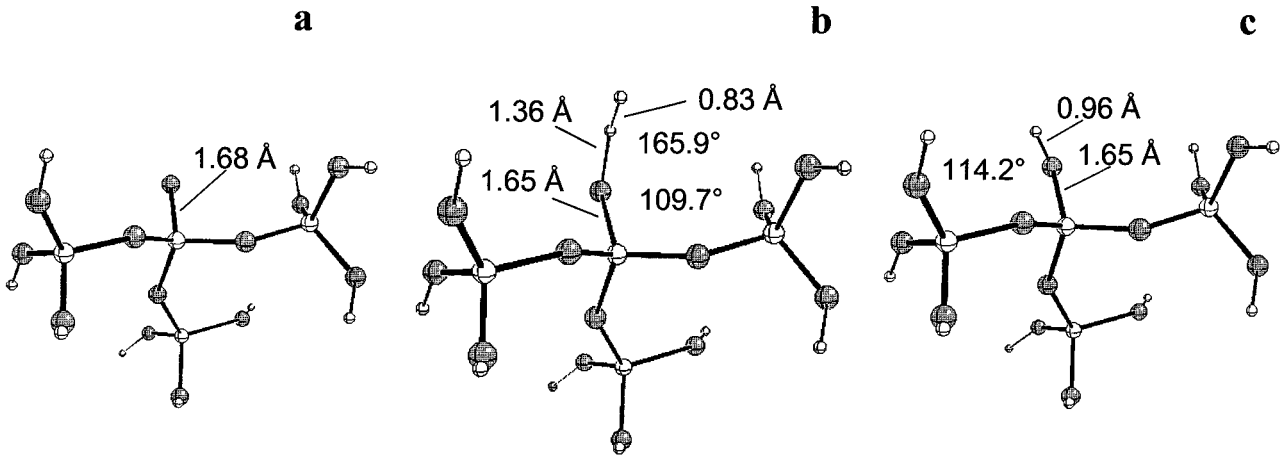

Figure 4. 4-Tetrahedron (4T) cluster model of a nonbridging oxygen (NBO) reacting with H_2: (a) ≡Si−O• center; (b) transition state ≡Si−O• + H_2; (c) ≡Si−OH center.

inherent to the models used, like the long-range polarization of the lattice and neglect of the long-range contribution of the Madelung potential, or to the method, like completeness of the basis set, validity of the exchange-correlation functional, quantum effects in hydrogen motion, etc. Because of all these limitations, the computed energy differences and barriers have to be considered with some care.

The calculations have been performed using the Gaussian94 program package.[33]

3. Results Discussion

3.1. H_2 Cracking at E′ Center. The isolated fragments giving rise to the reaction 1, ≡Si• and H_2, and the reaction products, ≡Si−H + H•, have been fully optimized separately. This provides the energy data to obtain thermodynamic information about the reaction. Using the 1T minimum model, Figure 1, we found that the ≡Si−H + H• system is 0.55 eV less stable than the ≡Si• + H_2 one, indicating that cracking of the H_2 molecule is slightly endothermic. Still, the energy required is easily accessible in high-temperature treatments. Much more complex is the determination of the transition state, TS, and of the corresponding energy barrier. To identify the structure of the TS we first performed a scan of the potential energy surface, Figure 8. The surface has been determined by imposing the H−H axis to be collinear with the ≡Si−H bond of the resulting fragment, as shown in Scheme 1; the two geometrical parameters

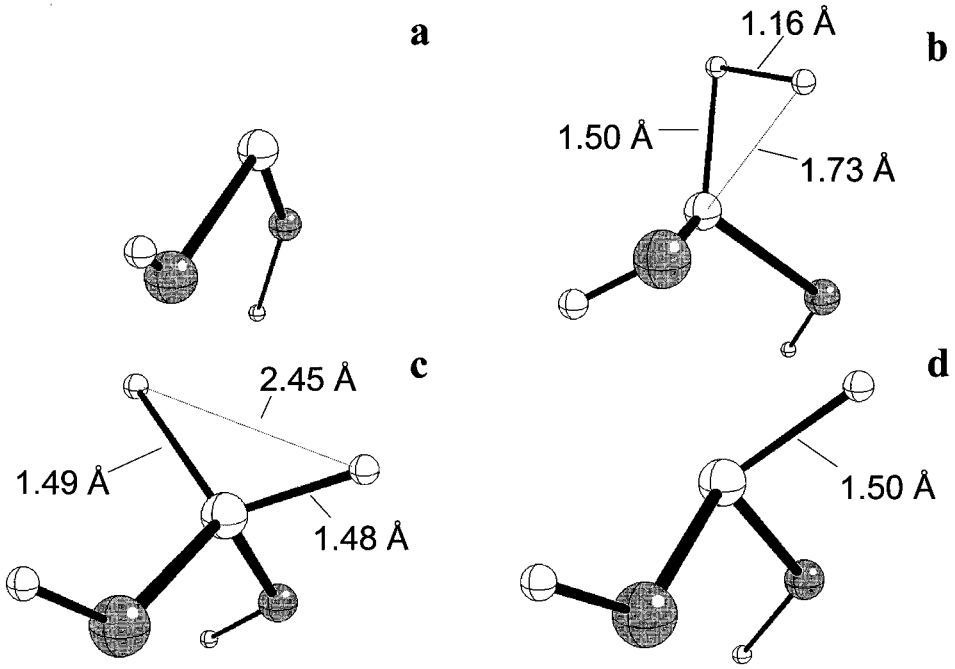

Figure 5. Cluster model of a dicoordinated Si reacting with H_2: (a) $=Si:$ center; (b) transition state $=Si: + H_2$; (c) $=Si(H)_2$ center; (d) $[=Si-H]^{\bullet}$ center.

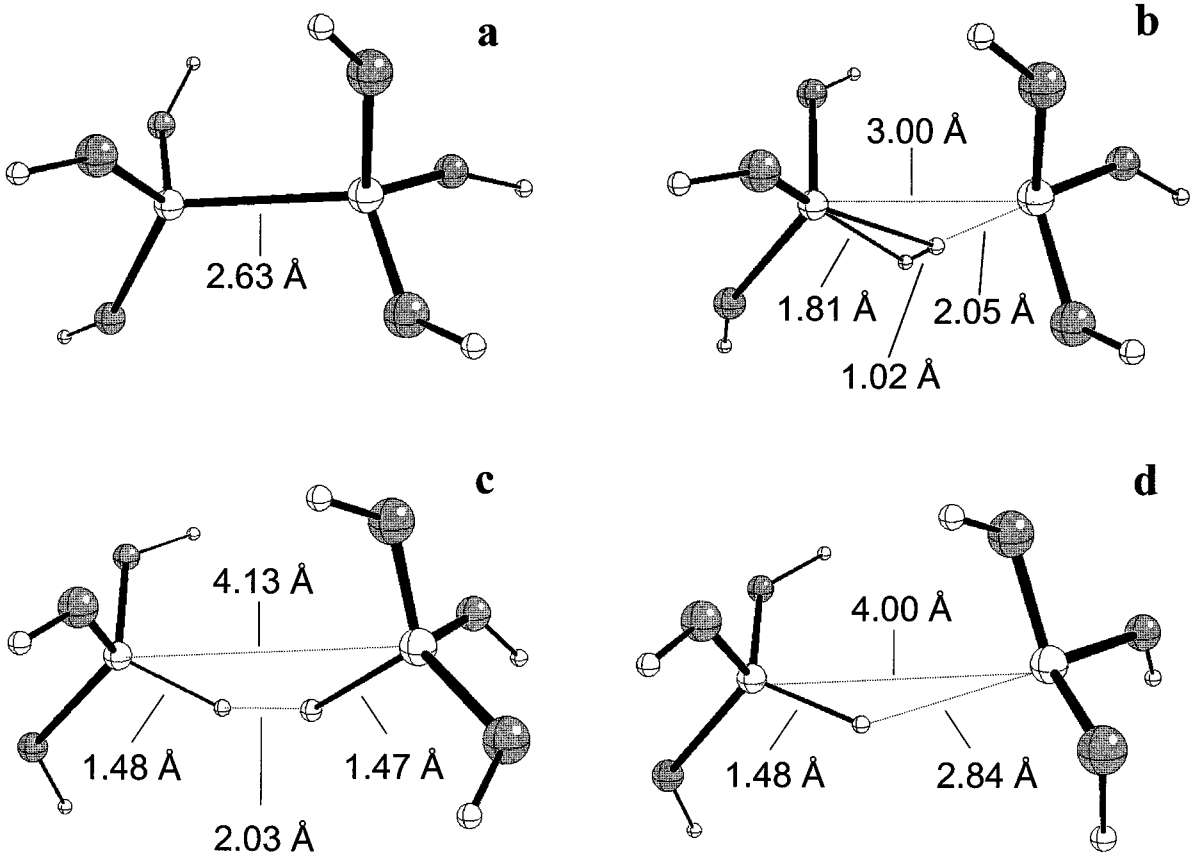

Figure 6. Small cluster model of an oxygen vacancy reacting with H_2: (a) $\equiv Si-Si\equiv$ center; (b) transition state $\equiv Si-Si\equiv + H_2$; (c) $\equiv Si-H$ $H-Si\equiv$ center; (d) $\equiv Si-H$ $^{\bullet}Si\equiv$ center.

that have been varied are therefore $r(Si-H_a)$ and $r(H_a-H_b)$.

From Figure 8, one sees that the potential is rather flat and the saddle point is close to $r(Si-H_a) \approx 1.6$ Å, and $r(H_a-H_b) \approx 1.25$ Å; a rough estimate of the activation energy is $E_a \approx 0.58$ eV. This shows that the TS is sufficiently similar to the final products of the reaction.

A real search for the TS has been performed using the Peng et al. algorithm.[34] The starting geometry has been assembled using the fully optimized $\equiv Si-H$ cluster geometry, Figure 1c, $r(Si-H_a) = 1.49$ Å, and positioning H_b at 0.9 Å from H_a. The search of the TS has been successful, leading to a structure with $Si-H_a$ and H_a-H_b distances of 1.56 and 1.31 Å, respectively, Figure 1b. The resulting activation energy value is $E_a = 0.58$ eV, which is almost identical to the value deduced from the

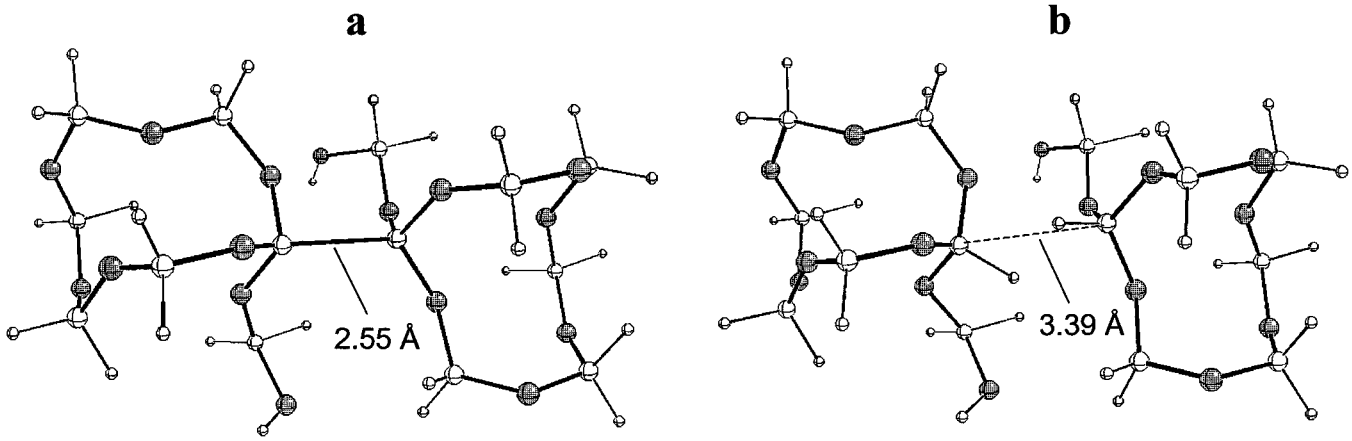

Figure 7. Large cluster model of an oxygen vacancy reacting with H_2: (a) ≡Si−Si≡ center; (b) ≡Si−H H−Si≡ center.

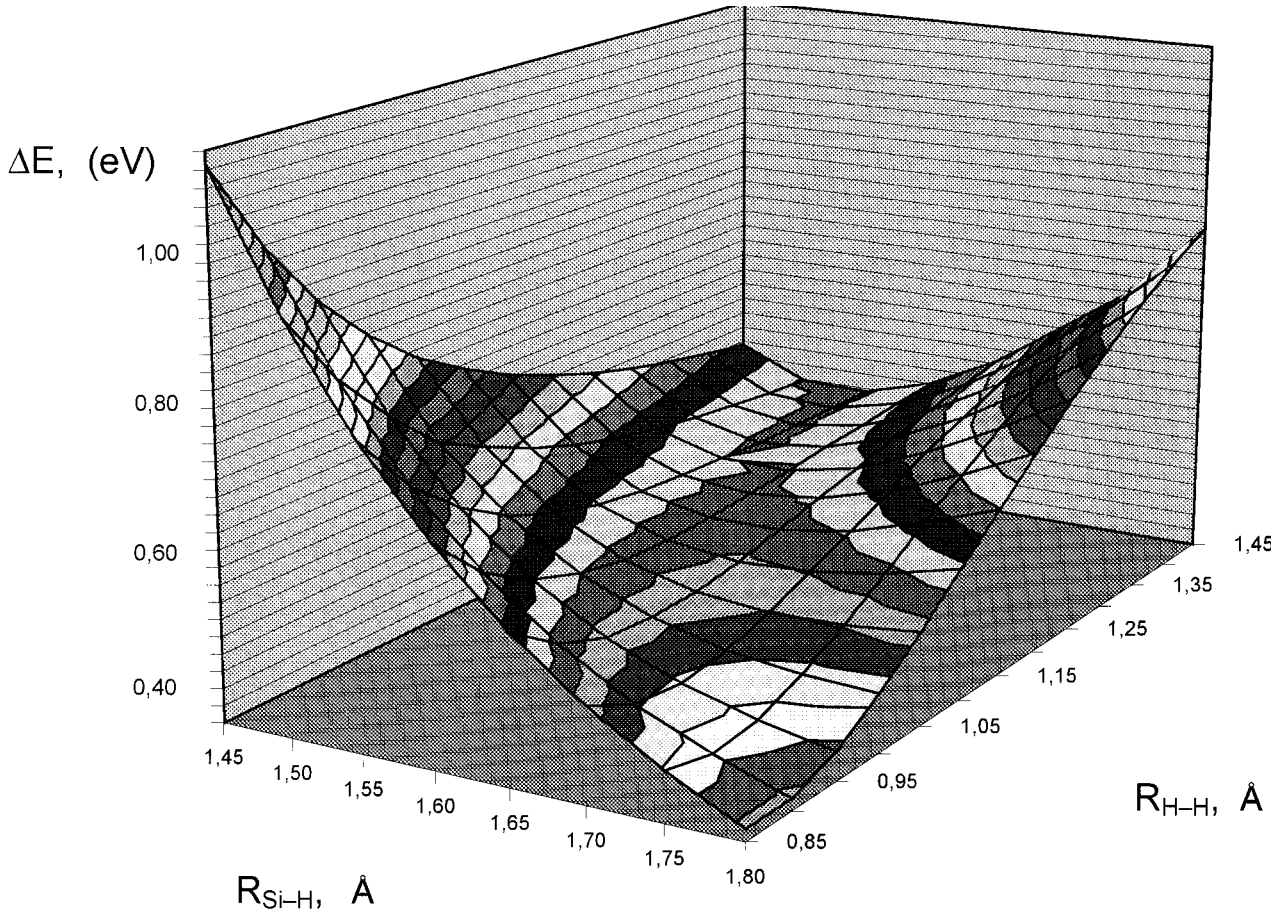

Figure 8. Potential energy surface for the reaction ≡Si• + H_2 → ≡Si−H + H•; only two geometrical parameters have been varied, *r*(Si−H) and *r*(H−H). The energy differences, Δ*E*, are given with respect to the total energy of the reactants, ≡Si• + H_2.

SCHEME 1

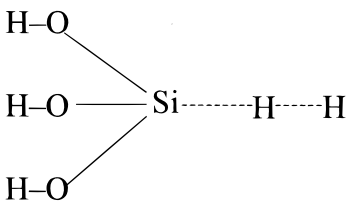

total energy surface scanning, Figure 8. This is only 0.03 eV higher than the energy required for the reaction, 0.55 eV. This means that the reverse process, ≡Si−H + H• → ≡Si• + H_2, is exothermic and has a very small barrier. A schematic representation of the reaction path is shown in Figure 9. To make sure that the stationary point found in the calculation really corresponds to a TS we have performed a full vibrational analysis. We found only one negative (imaginary) frequency for the Si−H_b stretching mode, thus providing compelling evidence that the stationary point corresponds to the TS for reaction 1. Thus, the calculations predict that atomic hydrogen readily depassivates the ≡Si−H bonds forming Si dangling bonds, ≡Si•, and molecular hydrogen. Indeed the reaction is well documented at the Si/SiO_2 interface where neutral Si dangling bonds have been detected by ESR and capacitance voltage methods.[35,36] There have been reports that the extraction

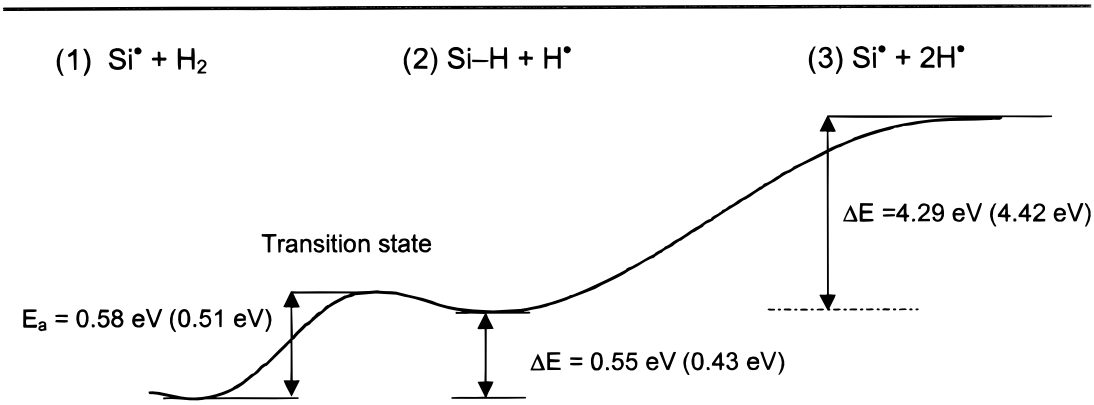

Figure 9. Energy profile for the reaction $\equiv Si^{\bullet} + H_2 \rightarrow \equiv Si-H + H^{\bullet} \rightarrow \equiv Si^{\bullet} + 2H^{\bullet}$. Energy values obtained with the 1T model; in parentheses are given the energy values computed with the 4T model.

of H by H atoms from the ≡Si−H groups is exothermic with a very small energy barrier, in full agreement with the present results.[37]

These results have been carefully checked as a function of cluster size by repeating the calculations using the 4T model, Figure 2. From the thermodynamic point of view, we found that the endothermicity of the process is reduced, from 0.55 to 0.43 eV, Figure 9. To reduce the computation effort, the OH groups of the 4T model were fixed during the TS search. However, the search for the TS leads to a similar structure as found with the 1T model, with $Si-H_a$ and H_a-H_b distances of 1.57 and 1.23 Å, respectively, Figure 2b. The corresponding energy barrier is slightly smaller, 0.51 eV, but still close to that obtained with the minimum cluster. These calculations do note take into account nonadiabatic effects which can be of considerable importance given the relatively high zero-point energy of the hydrogen molecule, about 0.3 eV. Indeed, Edwards has shown recently[9] that nonadiabatic terms can lower the computed barriers for hydrogen dissociation by 0.4 eV. Other groups have recently estimated nonadiabatic effect to be of the order of 0.2 eV only.[38] Thus, our computed adiabatic values of the energy barriers must be considered as upper bounds to the real values.

There have been a number of reports indicating that the E′ center is responsible for hydrogen dissociation, but the issue has been rather controversial. Recently, Conley and Lenahan[1,2] concluded that the E′/H_2 reaction occurs quite rapidly in novel as well as in thermally grown oxides. In a similar way, Li et al.[11] saw an E′ density decrease with room temperature H_2 exposure. The H_2 dissociation at E′ centers in bulk silica or at the silica surface is also the only one for which experimental estimates of the activation barrier have been reported. Li et al. have found $E_a \approx 0.3$ eV for thermal oxide, and Radzig and co-workers[12] have found a barrier of 0.43 ± 0.04 eV on the surface of reactive silica. Our computed values are very close to the experimental estimates, in particular if one considers the absence of nonadiabatic effects. From these values, one can conclude that the chemical reaction between the E′ centers and hydrogen will take place only at room or higher temperatures. On the other hand, we have shown that the reverse process, creation of Si dangling bonds, occurs easily when atomic H reacts with the silane groups. From the computational point of view we have to mention that the present results are close to those obtained by Edwards et al.;[39] using a similar basis set and a correlated MP2 wave function these authors found a barrier for reaction 1 of 0.72 eV.[39]

Another important process which has been considered here is

$$\equiv Si-H \rightarrow \equiv Si^{\bullet} + H^{\bullet} \qquad (5)$$

which provides a direct estimate of the strength of the Si−H bond. The two clusters, 1T and 4T, give again similar energies for this highly endothermic process, 4.29 and 4.42 eV, respectively. These values are in line with previously reported experimental and theoretical estimates. The strength of the bond is large enough to conclude that high-energy photons in the UV region of the spectrum are required. Actually, the ≡Si−H bond in silica shows absorption bands around 7.6 eV;[23,40] photons of this energy can therefore lead to a homolytic rupture of the Si−H bond and to the release of atomic H in the lattice. It should be mentioned that the cost for reaction 5 could significantly decrease if the H atom which forms during the process simultaneously reacts with another site to form a new bond. Indeed, there have been reports that the energetic cost of breaking the Si−H bond in solid SiO_2 is lower than in the gas-phase.[41]

3.2. H_2 Cracking at NBO Center. As opposed to reaction 1, the interaction of H_2 with a NBO center leading to the formation of an hydroxyl group, ≡Si−OH, is exothermic according to the DFT-B3LYP calculations. Also in this case, the calculations have been performed with the 1T and the 4T cluster models, Figures 3 and 4, respectively, but the energy released in the reaction is practically the same, 0.38 and 0.40 eV, respectively. This is a very important result which strongly indicates the NBO center as one of the key sites for hydrogen cracking in silica. The accurate determination of the activation barrier becomes even more important than for the E′ center since the favorable thermodynamic balance does not necessarily imply a kinetically accessible process.

To identify the TS, we first performed a scan of the potential energy surface keeping some geometrical parameters fixed and varying the most crucial parameters for the reaction, i.e., the $O-H_a$ and the H_a-H_b bonds. The scan has been done with the smaller 1T model. The H−H bond has been imposed to be collinear with the O−H bond of the ≡Si−O−H final product; see Scheme 2.

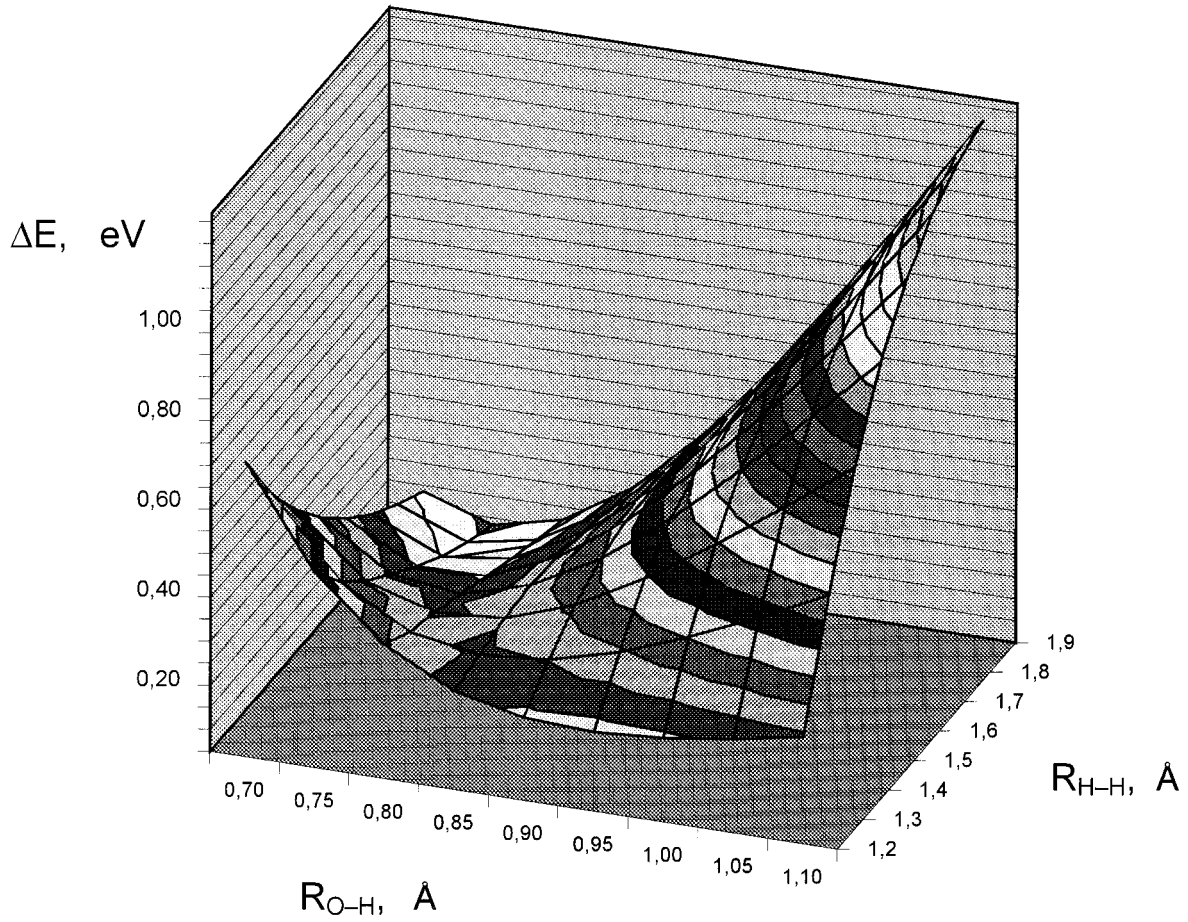

Figure 10. Potential energy surface for the reaction $\equiv Si-O^{\bullet} + H_2 \rightarrow \equiv Si-OH + H^{\bullet}$; only two geometrical parameters have been varied, r(O−H) and r(H−H). The energy differences, ΔE, are given with respect to the total energy of the reactants, $\equiv Si-O^{\bullet} + H_2$.

SCHEME 2

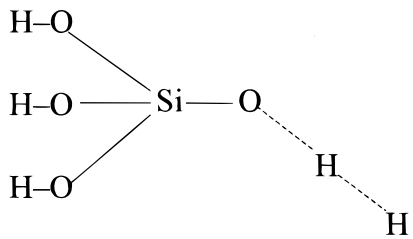

From the energy surface, shown in Figure 10, the transition state is found to be close to $r(O-H_a) \approx 1.5$ Å and $r(H_a-H_b) \approx 0.85$ Å; at this geometry, the total energy is about 0.3 eV higher than the energy of the noninteracting $\equiv Si-O^{\bullet}$ and H_2 fragments.

The full localization of the TS has been performed starting from this geometry and leads to a stationary point where the optimal $O-H_a$ and H_a-H_b distances are of 1.35 and 0.83 Å, respectively, Figure 3b. The TS nature of the stationary point has been verified by performing a full vibrational analysis. We obtained a single negative frequency corresponding to the $O-H_b$ stretching, thus confirming that the geometry is that of a saddle point. The energy of the TS is only 0.15 eV above that of the reactants. Thus, the activation energy for reaction 2 is very low, well below that found for the E′ center and such that H_2 cracking at NBO centers can occur even below room temperature. Given the very low computed barrier and the absence of nonadiabatic terms, it is likely that the wave function tunnels readily through the barrier between the two wells. A summary of the energetics for reaction 2 is given in Figure 11. As for the E′ case, we have shown in parenthesis the energy values computed with the larger 4T cluster. The results are very satisfactory since the barrier decreases by only 0.02 eV with the larger model, Figure 11. Not only the energies but also the geometries are similar; in the TS computed with the 4T model $r(O-H_a) = 1.36$ Å and $r(H_a-H_b) = 0.83$ Å, Figure 4b, are very close to the values obtained with the 1T cluster, Figure 3b.

We have also considered the process

$$\equiv Si-O-H \rightarrow \equiv Si-O^{\bullet} + H^{\bullet} \qquad (6)$$

with breaking of the O−H bond; this requires about 5.2 eV. Again, notice the very similar values found with the two clusters, Figure 11. Thus, the energy needed to dissociate the O−H bonds is even higher than for the Si−H bonds. Notice that the energy of reaction 6 is lower than that involved in the dissociation of the $\equiv Si-O-H$ bond into $\equiv Si^{\bullet} + OH^{\bullet}$; this latter process in fact requires 5.8 eV according to our calculations.

Recent experiments suggest that H_2 cracking is due to surface NBO centers created by breaking the Si−OH surface groups.[42] The processes and the corresponding energy changes, are $\equiv Si-OH \rightarrow \equiv Si-O^{\bullet} + H^{\bullet}$ with $\Delta E = 5.2$ eV and $\equiv Si-O^{\bullet} + H_2 \rightarrow \equiv Si-OH + H^{\bullet}$ with $\Delta E = -0.4$ eV. In this global process, the $\equiv Si-O^{\bullet}$ groups are formed at high temperatures, around 1000 K, at the expense of the $\equiv Si-OH$ groups, but then act as "catalytic" centers for further cracking of incoming hydrogen molecules. The process releases atomic hydrogen which, at these temperatures, is not trapped at the defect sites but diffuses rapidly into the bulk material.

3.3. H_2 Cracking at Dicoordinated Si. The results of the previous sections have shown that the interaction of molecular

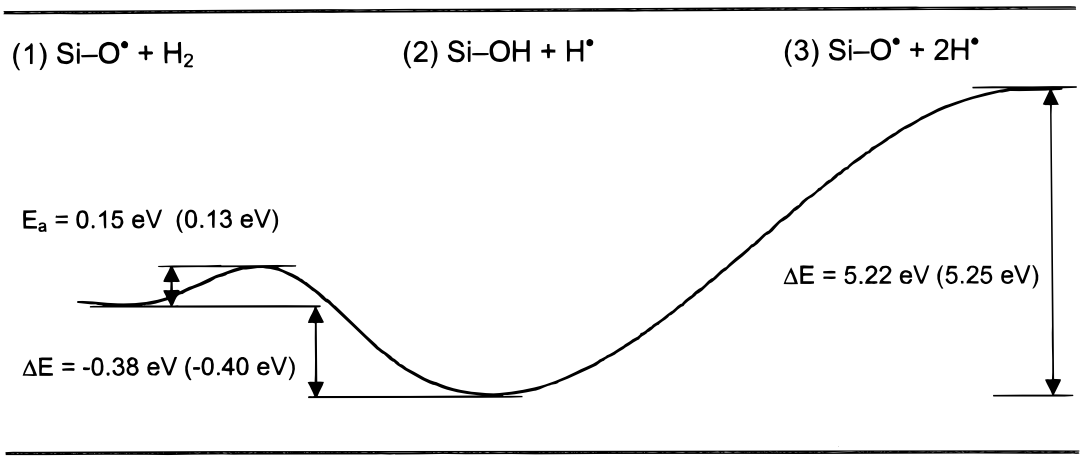

Figure 11. Energy profile for the reaction ≡Si−O• + H_2 → ≡Si−OH + H• → ≡Si−O• + 2H•. Energy values obtained with the 1T model; in parentheses are given the energy values computed with the 4T model.

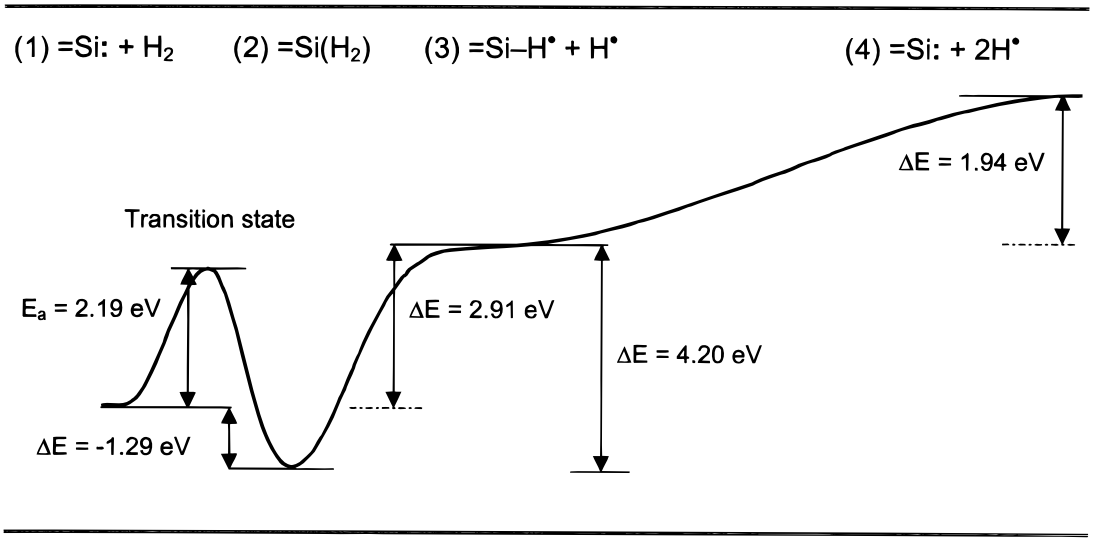

Figure 12. Energy profile for the reaction =Si: + H_2 → ≡$Si(H)_2$ → [=Si−H]• + H• → =Si: + 2H•.

hydrogen with the E′ and NBO centers depends on the first neighbors only and that very similar results are obtained with clusters of different size. For this reason, we decided to use only the small $(HO)_2Si$ cluster to study reaction 3 where hydrogen dissociates at a dicoordinated Si center with formation of two Si−H bonds; see Figure 5a. The first important result is that the process is exothermic by 1.29 eV as a result of the formation of two Si−H bonds at the expense of the H−H bond which has a $D_e = 4.84$ eV and a $D_0 = 4.57$ eV according to our calculations (the experimental value for H_2 is $D_0 = 4.45$ eV).[43] The reaction, however, is accompanied by a relatively large barrier of 2.19 eV; see Figure 12. The structure of the TS is shown in Figure 5b along with the main geometrical parameters. As for the previous cases, the TS nature has been checked by performing a full vibrational analysis. Clearly, the cracking of hydrogen can occur at these diamagnetic sites only at relatively high temperatures.

Recently, Zhang and Raghavachari[44] have studied the addition of H_2 to a dicoordinated Ge atom in Ge-doped silica using a similar computational approach to ours. They found that the reaction is exothermic by 0.4 eV, i.e., less than for the Si case where we found a ΔE of −1.3 eV, Figure 12, and has a barrier of 2.8 eV, somewhat higher than for =Si: where $E_a = 2.2$ eV. The structure of the TS is also similar, with Ge−H and H−H distances which are about 0.1 Å longer than in the Si case; compare Figure 5b with Figure 1b in ref 44. In a recent study, Radzig and co-workers[12] have studied in detail the kinetics of the cracking reaction of H_2 at a dicoordinated Si center. They found that this type of oxygen deficient center does not react with H_2 under normal conditions ($T = 300$ K and $P(H_2) = 100$ Torr) and that even at $T = 900$ K the reaction rate constant is of the order of 10^{-17} cm^3/(molecule s). On the basis of this observation, they concluded that the activation energy for reaction 3 is not less than 1.3 eV; our calculations give $E_a \approx 2.2$ eV. It is important to mention that when the sample is irradiated with UV light the barrier drops dramatically since the reaction becomes photoinduced and involves the excited singlet or triplet states of the dicoordinated Si center. In fact, the estimated activation energy is, in this case, of the order of 0.04 eV for the singlet and 0.2 eV for triplet excited states.[12]

An alternative path for the reaction could be the following:

$$=Si: + H_2 \rightarrow [=Si-H]^\bullet + H^\bullet \qquad (7)$$

in which the H_2 forms only one Si−H bond and leads to the formation of atomic hydrogen. The optimal structure of the [=Si−H]• fragment is shown in Figure 5d. However, as can be seen from Figure 12, the process is endothermic by 2.91 eV and, more important, the energy of the products of reaction 7 is higher than that of the TS of reaction 3. Thus, reaction 7 is

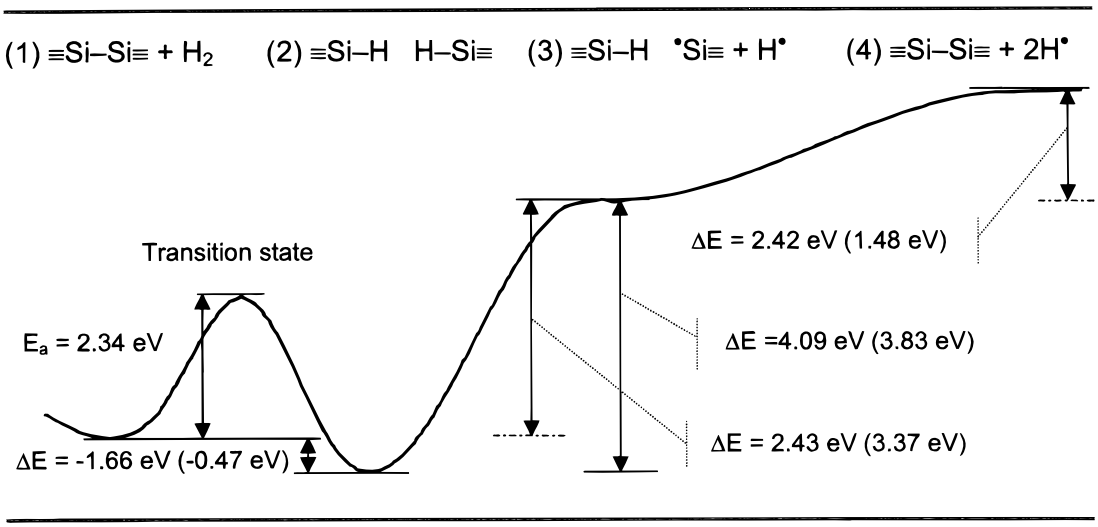

Figure 13. Energy profile for the reaction ≡Si−Si≡ + H_2 → ≡Si−H H−Si≡ → ≡Si−H + •Si≡ + H• → ≡Si−Si≡ + 2H• (small cluster results); in parentheses are given the energy values computed with the large cluster, Figure 7a.

unlikely to occur unless the H atom which is produced binds at the same time to another site.

Finally, it is interesting to comment on the relative strength of the Si−H bond in ═Si(H_2), Figure 5c, compared to ≡Si−H, Figure 1c, where the Si atom is bonded to three instead of two oxygen neighbors. However, this seems to have very little effect on the first Si−H dissociation energy which in ═Si$(H)_2$ is 4.29 eV, almost exactly the same value found for the breaking of the ≡Si−H bond; see Figure 9. The breaking of the second Si−H bond, however, corresponding to the following process

$$\text{═Si−H}^{\bullet} \rightarrow \text{═Si:} + \text{H}^{\bullet} \qquad (8)$$

requires only 1.94 eV, Figure 12. This means that a free H atom could easily extract a bonded H atom from the ═Si−H• center to form the H_2 molecule and leaving the di-coordinated Si center; this is the reverse of reaction 7 and corresponds indeed to an energy gain of almost 3 eV.

3.4. H_2 Cracking at an Oxygen Vacancy. A number of recent studies suggest that films of buried oxides deposited on Si contain excess Si in order to explain the enhanced sensitivity to E′ generation.[45−47] This excess Si leads to an increased density of neutral oxygen vacancies, ≡Si−Si≡, and it is generally accepted that these centers may serve as E′ and ≡Si−H bond precursors. Indeed, two processes have been postulated at different temperatures. At 750 K, the reaction proceeds by incorporation of a H atom in a ≡Si−Si≡ bond with release of a free electron and a neutral H atom and formation of a proton bridge,

$$\text{≡Si−Si≡} + \text{H}_2 \rightarrow [\text{≡Si−H−Si≡}]^{+} + \text{H}^{\bullet} + \text{e}^{-} \qquad (9)$$

The electrons can escape from the oxide to the Si conduction band leaving a positively charged but ESR-inactive center. At higher temperatures, above 1000 K, it has been suggested that reaction 4 takes place where H_2 is incorporated into the ≡Si−Si≡ bond with formation of two ≡Si−H units.[40] The occurrence of reaction 4 is shown by the appearance of a peak at 2250 cm^{-1} in the infrared absorption spectrum due to the ≡Si−H bond; furthermore, there is a decrease of the typical 7.6 eV optical absorption band due to a neutral oxygen vacancy. Reaction 4 is believed to convert all ≡Si−Si≡ precursor centers in neutral ≡Si−H bonds around 1000 K, thus preventing the activation of the positively charged state (the proton bridge). Dissociation in vacuum of the ≡Si−H neutral state occurs at $T \approx 1300$ K and most probably proceeds as the reverse of reaction 4. Thus, the interaction of molecular hydrogen with this defect center may lead in principle to the formation of two silane groups, ≡Si−H, or to a structure where one H atoms replaces the bridging oxygen in the regular network, [≡Si−H−Si≡]•, also known as the neutral hydrogen bridge in quartz and attributed to the E'_4 center.[48] In this latter case, the reaction is

$$\text{≡Si−Si≡} + \text{H}_2 \rightarrow [\text{≡Si−H−Si≡}]^{\bullet} + \text{H}^{\bullet} \qquad (10)$$

A neutral oxygen vacancy in silica is formed by removing a bridging oxygen atom from a ≡Si−O−Si≡ bond; the recombination of the two ≡Si • dangling bonds results in a new, direct, Si−Si bond and in a substantial relaxation of the structure. The Si−Si distance, which is of 3.06 Å in α-quartz, decreases to ∼2.5 Å. To model the oxygen vacancy we used two clusters, a small one, $(HO)_3$Si−Si$(OH)_3$, Figure 6a, and a larger one, Figure 7a. A search of the transition states has been attempted only for the smaller model. We first analyzed the structure of the final products of the reactions 4 and 10; in the calculations, we always maintained fixed the positions of the saturating H atoms of the clusters.

We performed a first geometrical optimization placing an H atom along the Si−Si bond of the oxygen vacancy (product of reaction 10). The system has an odd number of electrons, and we considered a doublet spin state. The Si−Si distance, which is ∼2.6 Å initially, increases considerably, and the system undergoes a strong distortion. The H atom binds to only one Si atom, with a Si−H distance of 1.48 Å, and is separated by 2.84 Å from the second one, Figure 6d. As a consequence, the unpaired electron is entirely localized on the second Si, as shown also by the value of the Fermi contact term and of the corresponding hyperfine coupling constant with the ^{29}Si nuclide, 284 G, which is very close to that obtained with a 1T model of the E′ center, ≡Si•, 273 G. This center is thus ESR visible and corresponds to the E'_4 center in α-quartz and to the E'_β center in amorphous silica.[49,50]

The formation of two silane groups starting from an O vacancy has been described by placing an H_2 molecule with r(H−H) = 0.7 Å into the Si−Si bond; the geometry optimization leads to two ≡Si−H groups, with similar Si−H distances, ∼1.47 Å, and a large Si−Si distance of 4.13 Å, Figure 6c. The distance

between the two ≡Si−H groups is much shorter in the larger model, which shows a Si−Si distance of 3.4 Å, Figure 7b. The local coordination around each Si is pseudotetrahedral and very similar to what is found when an isolated H atom passivates a ≡Si• dangling bond. Since the space in the cavity left by the missing oxygen is not large, the two ≡Si−H groups give rise to a considerable repulsion which results in a distortion of the structure. The relaxation following the formation of the Si−H bonds is described differently with the two clusters used, and correspondingly, the energetics are quite different in the two cases. Of course, the larger model is expected to give more reliable energy differences.

The relative energies of the species involved in reactions 4 and 10 are shown in Figure 13. According to the DFT-B3LYP results, the cracking of H_2 at an oxygen vacancy and the formation of two silane groups is a process which is thermodynamically favorable by ∼0.5 eV (1.7 eV with the small model). Given the large relaxation involved in the H_2 addition process, the small cluster model does not provide adequate answers. We also computed the energy barrier for the H_2 breaking reaction 4. The search for the TS started from a geometry intermediate between that of reactants and products and was done using only the small cluster. The calculation leads to a stationary point which, according to the vibrational analysis, corresponds to a TS with these geometrical characteristics: $r(Si-Si) \approx 3.0$ Å; $r(Si_a-H_a) \approx 2.1$ Å; $r(Si_b-H_b) \approx 1.8$ Å; $r(H-H) \approx 1.0$ Å, Figure 6b. The corresponding activation energy, 2.34 eV, is rather large, one of the largest computed here. This suggests that breaking the H_2 molecule at the V_O sites is only possible at high temperatures but is not expected to occur at room temperature, in agreement with the experimental observations. Once the ≡Si−H is formed, the energy required to break it is practically the same computed with the other cluster models; see Figure 9, i.e., about 4 eV. Again, the bond energy is practically independent of the size of the cluster and on the substituents. It only reflects the local nature of the Si−H covalent bond.

4. Conclusions

We have studied the interaction and the dissociation mechanism of H_2 at point defects in SiO_2 by means of gradient-corrected density functional theory calculations and cluster models. The energy of the reactants and of the products and the corresponding activation energies and transition states have been determined for the following defect sites: ≡Si•, a Si singly occupied sp^3 dangling bond (E′ center), ≡Si−O•, a nonbridging oxygen center, =Si**:** or divalent Si, and ≡Si−Si≡, the neutral oxygen vacancy. We used clusters of various size but we found that the energetics is very similar whether small or large clusters are used, in line with previous observations of a strong localization of the bonding electrons in the silica network.

H_2 cracking on the NBO sites is found to be exothermic by ∼0.4 eV; the H−H dissociation process implies an energy barrier of ∼0.1 eV only, which strongly indicates this center as one of the most important for H_2 cracking at low temperature, well below room temperature. The value of the barrier is very small and since the zero-point energy of the H_2 molecule is so large, spontaneous dissociation can occur at these sites. On a Si dangling bond, the formation of ≡Si−H and a neutral H atom is an endothermic process that requires overcoming a barrier of 0.5 eV, again an upper bound because of the absence of nonadiabatic effects. Thus, Si dangling bonds are expected to induce the hydrogen cracking at room temperatures or higher.

The interaction of molecular hydrogen with two diamagnetic oxygen deficient centers, =Si**:** and ≡Si−Si≡, leads to the formation of stable ≡Si−H groups with an exothermic process but involves relatively high activation energies of the order of 2 eV. In conclusion, H_2 cracking is predicted to occur at room temperature on paramagnetic defects (more easily on the nonbridging oxygens) and at high temperatures of the diamagnetic centers.

Acknowledgment. The authors thank Rod Devine for the stimulating discussions and the critical reading of the manuscirpt. Financial support from the Spanish "Ministerio de Educación y Ciencia", Project CICyT PB95-0847-C02-01, "Acción Integrada Hispano-Italiana, HI1998-0042", "Generalitat de Catalunya" Projects 1997SGR00167, the Italian INFM (Project PAIS) is acknowledged. Part of the computer time was provided by the "Centre de Supercomputació de Catalunya", CESCA, and Centre Europeu de Parallelisme de Barcelona, CEPBA, through a research grant of the University of Barcelona and through the Training and Mobility of Researchers (TMR) program of the European Committee under Contract ERB FMGE CT95 0062. M. Vitiello thanks the TMR program for supporting his stays at the University of Barcelona.

References and Notes

(1) Conley, J. F.; Lenahan, P. M. *Appl. Phys. Lett.* **1993**, *62*, 40.
(2) Conley, J. F.; Lenahan, P. M. *IEEE Trans. Nucl. Sci.* **1993**, *41*, 1335.
(3) Stahlbush, R. E.; Edwards, A. H.; Griscom, D. L.; Mrstik, B. J. *J. Appl. Phys.* **1993**, *73*, 658.
(4) DiMaria, D. J.; Stasiak, J. W. *J. Appl. Phys.* **1989**, *65*, 2342.
(5) Griscom, D. L. *J. Non-Cryst. Solids* **1985**, *73*, 51.
(6) Skuja, L. *J. Non-Cryst. Solids* **1998**, *239*, 16.
(7) Vanheusden, K.; Warren, W. L.; Devine, R. A. B.; Fleetwood, D. M.; Schwank, J. R.; Schaneyfelt, M. R.; Winokur, P. S.; Lemnios, Z. J. *Nature* **1997**, *386*, 587.
(8) Atkins, A. M.; Lemaire, P. J.; Erdogan, T.; Mizrahi, V. *Electron. Lett.* **1993**, *29*, 1234.
(9) Edwards, A. H. *J. Non-Cryst. Solids* **1995**, *187*, 232.
(10) Stahlbush, R. E.; Lawrence, R. K.; Richards, W. *IEEE Trans. Nucl. Sci.* **1989**, *NS36*, 1998.
(11) Li, Z.; Fonash, S. J.; Poindexter, E. H.; Harmatz, M.; Rong, F.; Buchwald, W. R: *J. Non-Cryst. Solids* **1990**, *126*, 173.
(12) Radzig, V. A.; Bagratashvili, V. N.; Tsypina, V. I.; Chernov, P. V.; Rybaltovskii, A. O. *J. Phys. Chem.* **1995**, *99*, 6640.
(13) Radtsig, V. A. *Chem. Phys. Rep.* **1995**, *14*, 1206.
(14) Xu, X.; Goodman, D. W. *Appl. Phys. Lett.* **1992**, *61*, 774.
(15) Bart, F.; Gautier, M.; Jollet, F.; Durand, J. P. *Surf. Sci.* **1994**, *306*, 342.
(16) Le Page, Y.; Calvert, L. D.; Gabe, E. J. *J. Phys. Chem. Solids* **1980**, *41*, 721.
(17) Lopez, N.; Pacchioni, G.; Maseras, F.; Illas, F. *Chem. Phys. Lett.* **1998**, *294*, 611.
(18) Pacchioni, G.; Ieranò, G. *Phys. Rev. B* **1997**, *56*, 7304.
(19) Pacchioni, G.; Vitiello, M. *Phys. Rev. B* **1998**, *58*, 7745.
(20) Pacchioni, G.; Ieranò, G.; Marquez, A. M. *Phys. Rev. Lett.* **1998**, *81*, 377.
(21) Hamann, D. R. *Phys. Rev. Lett.* **1998**, *81*, 3447.
(22) Boero, M.; Pasquarello, A.; Sarthein, J.; Car, R. *Phys. Rev. Lett.* **1997**, *78*, 887.
(23) Pacchioni, G.; Ieranò, G. *Phys. Rev. B* **1998**, *57*, 818.
(24) Pacchioni, G.; Ferrario, R. *Phys. Rev. B* **1998**, *58*, 6090.
(25) Pacchioni, G.; Ieranò, G. *Phys. Rev. Lett.* **1997**, *79*, 753.
(26) Stefanov, B. B.; Raghavachari, K. *Phys. Rev. B* **1997**, *56*, 5035.
(27) Zhang, B. L.; Raghavachari, K. *Phys. Rev. B* **1997**, *55*, R15993.
(28) Becke, A. D. *J. Chem. Phys.* **1993**, *98*, 5648.
(29) Lee, C.; Yang, W.; Parr, R. G. *Phys. Rev. B* **1982**, *37*, 785.
(30) Franci, M. M.; Pietro, W. J.; Hehre, W. J.; Binkley, J. S.; Gordon, M. S.; DeFrees, D. J.; Pople, J. A. *J. Chem. Phys.* **1982**, *77*, 3654.
(31) Gordon, M. S.; Binkley, J. S.; Pople, J. A.; Pietro, W. J.; Hehre, W. J. *J. Am. Chem. Soc.* **1982**, *104*, 2797.
(32) Curtiss, L. A:; Raghavachari, K.; Redfern, P. C.; Pople, J. A. *J. Chem. Phys.* **1997**, *106*, 1063.
(33) Frisch, M. J., et al. *Gaussian 94*; Gaussian Inc.: Pittsburgh, PA, 1997.
(34) Peng, C.; Ayala, P. J.; Schlegel, H. B.; Frisch, M. J. *J. Comput. Chem.* **1996**, *17*, 49.
(35) Cartier, E.; Stathis, J. H. *Microelectron. Eng.* **1995**, *28*, 3.

(36) Di Maria, D. J. *Microelectron. Eng.* **1995**, *28*, 63.
(37) Lucovsky, G.; Yang, H.; Jing, Z.; Whitten, J. L. *Appl. Surf. Sci.* **1997**, *117/118*, 192.
(38) Kurtz, H.; Karna, S. Personal communication.
(39) Edwards, A. H.; Pickard, J. A.; Stahlbush, R. E. *J. Non-Cryst. Solids* **1994**, *179*, 148.
(40) Imai, H.; Arai, K.; Hosono, H.; Abe, Y.; Arai, T.; Imagawa, H. *Phys. Rev. B* **1991**, *44*, 4812.
(41) Jennison, D. R.; Sullivan, J. P.; Schultz, P. A.; Sears, M. P.; Stechel, E. B. *Surf. Sci.* **1997**, *390*, 112.
(42) Devine, R. A. B. Personal communication.
(43) Hubert, K.; Herzberg, R. G. *Molecular Spectra and Molecular Structure − Constants of Diatomic Molecules*; Van Nostrand: New York, 1979.
(44) Zhang, B. L.; Raghavachari, K. *Phys. Rev. B* **1995**, *51*, 7946.
(45) Devine, R. A. B.; Leray, J. L.; Margail, J. *Appl. Phys. Lett.* **1991**, *59*, 2275.
(46) Vanheusden, K.; Stesmans, A. *J. Appl. Phys.* **1993**, *74*, 275.
(47) Vanheusden, K.; Stesmans, A. *Appl. Phys. Lett.* **1994**, *64*, 2575.
(48) Isoya, J.; Weil, J. A.; Halliburton, L. E. *J. Chem. Phys.* **1981**, *74*, 5436.
(49) Rudra, J. K.; Fowler, W. B.; Feigl, F. *Phys. Rev. Lett.* **1985**, *55*, 2614.
(50) Weeks, R. A. *J. Non-Cryst. Solids* **1994**, *179*, 1.